Photoproduction of isolated photons at HERA in NLO QCD

Maria Krawczyk

Institute of Theoretical Physics, Warsaw University, ul. Hoza 69, 00-681 Warsaw, Poland

E-mail: krawczyk@fuw.edu.pl

Abstract. The NLO QCD calculation for the photoproduction of an isolated photon with large p_T at the HERA ep collider is presented. The single resolved photon contribution and the QCD corrections of order α_s to the Born term are consistently included. The sizeable NNLO contributions, the box and the double resolved photon subprocesses, are in addition taken into account. The importance of the isolation cut as well as the influence of other experimental cuts on the p_T and η_γ distributions are discussed in detail. Results are compared with experimental data and with the different NLO calculations.

1. Introduction

The production in the ep collision of a prompt photon with large transverse momentum p_T is considered. Such a reaction is dominated by events with almost real photons mediating the ep interaction, $Q^2 \approx 0$, so in practice we deal with photoproduction of a prompt photon (called also Deep Inelastic Compton (DIC) scattering). The photon emitted by the electron may interact with the proton partons directly or as a resolved one. Analogously, the observed final photon may arise directly from hard partonic subprocesses or from fragmentation processes, where a quark or a gluon decays into γ.

The importance of the DIC process in the ep collision for testing the Parton Model and then Quantum Chromodynamics was studied previously by many authors [1]-[9]. Measurements were performed at the HERA ep collider by the ZEUS group [10]-[12], and [13], also the H1 Collaboration has presented preliminary results [14]. In these experiments events with isolated photons were included in the analysis, i.e. with a restriction imposed on the hadronic energy detected close to the photon. The corresponding cross sections for the photoproduction of an isolated photon and of an isolated photon plus jet were calculated in QCD in next-to-leading order (NLO) [15]-[22]. There exists an analogous calculation for the large-Q^2 case (DIS events) [23].

In this talk the results of the NLO QCD calculation for the DIC process with an isolated photon at the HERA ep collider are presented [18, 19]. We consider the parton distributions in the photon and parton fragmentation into the photon as quantities of

Figure 1. The Deep Inelastic Compton process (left) and Born process (right).

order α_{em}. We emphasize the importance of the box diagram $\gamma g \to \gamma g$, being the higher order process, in describing the data. Our approach differs from the NLO approach [15]-[17], [21, 22] by a set of subprocesses included in the analysis. The comparison of our predictions (KZ) [19] with the results obtained by L.E. Gordon (LG) [17] and M. Fontannaz et al. (FGH) [21] and with data measured by the ZEUS group [12] is presented.

2. The NLO calculation for $\gamma p \to \gamma X$ – general discussion

Different approaches to the NLO calculations of cross sections for hadronic processes involving resolved photons exist in the literature, see the discussion in [6, 18] and [24]. Here we discuss how the NLO QCD calculations, based on the DGLAP approach, are being performed for the DIC cross section (fig. 1, left),

$$\gamma p \to \gamma X, \tag{1}$$

where the final photon is produced with large transverse momentum, $p_T \gg \Lambda_{QCD}$.

The Born level contribution to the cross section for the DIC process (1), i.e. the term of lowest order in the strong coupling α_s, arises from the Compton process on the quark (fig. 1, right):

$$\gamma q \to \gamma q. \tag{2}$$

It gives the α_{em}^2 order contribution to the partonic cross section. At the same α_{em}^2 order it contributes to the hadronic cross section for the process $\gamma p \to \gamma X$. The Parton Model (PM) prediction for the DIC process (1), which applies for $x_T = 2p_T/\sqrt{S} \sim \mathcal{O}(1)$, relies solely on the Born contribution (2) [1], namely:

$$d\sigma^{\gamma p \to \gamma X} = \sum_q \int dx_p q_p(x_p) d\hat{\sigma}^{\gamma q \to \gamma q}, \tag{3}$$

where q_p is the quark density in the proton and $d\sigma^{\gamma p \to \gamma X}$ ($d\hat{\sigma}^{\gamma q \to \gamma q}$) stands for the hadronic (partonic) cross section. In the QCD improved PM the cross section is given by (3), however with scale dependent quark densities. For semihard processes, where $x_T \ll 1$, the prediction based on process (2) only is not a sufficient approximation, and one should also consider the contributions corresponding to the collinear showers, involving hadronic-like interactions of the photon(s). There are two classes of such

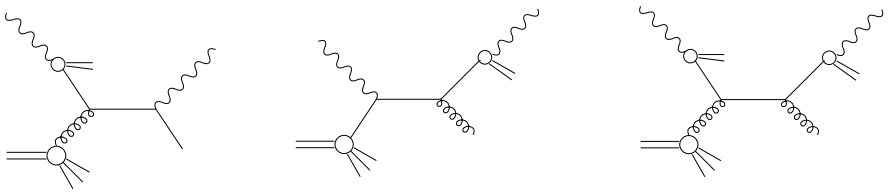

Figure 2. Examples of single resolved γ processes: the resolved initial photon (left) and the resolved final photon (center). An example of a double resolved photon process (right).

contributions: *single resolved* photon processes with resolved initial *or* final photon, and *double resolved* photon processes with both the initial *and* the final photon resolved (figs. 2). They correspond to partonic cross sections of orders $\alpha_{em}\alpha_s$ (single resolved) and α_s^2 (double resolved). If one takes into account that partonic densities in the photon and the parton fragmentation into the photon are of order $\sim \alpha_{em}$, then the contributions to the hadronic cross section from these resolved photon processes are $\alpha_{em}^2\alpha_s$ and $\alpha_{em}^2\alpha_s^2$, respectively. Both single and double resolved photon contributions are included in the standard LL QCD analyses of the DIC process [4, 5, 9]. To obtain the NLO QCD predictions for the process (1) the α_s corrections to the lowest order process (2) have to be calculated leading to terms of order $\alpha_{em}^2\alpha_s$ [4, 5, 25, 26] (fig. 3). In these $\alpha_{em}^2\alpha_s$ contributions there are collinear singularities to be subtracted and shifted into corresponding quark densities *or* fragmentation functions. This way the single resolved photon contribution appears in the calculation of the α_s corrections to the Born process. It is worth noticing that in the NLO expression for the cross section there are no collinear singularities which would lead to the double resolved photon contributions. It indicates that taking into account α_s^2 subprocesses, associated with both the initial and final photons resolved, goes beyond the accuracy of the NLO calculation. This will be consistent within the NNLO approach, where α_s^2 correction to the Born term and α_s correction to the single resolved terms should be included, all giving the same $\alpha_{em}^2\alpha_s^2$ order contribution to the hadronic cross sections.

The other set of diagrams is considered by some authors [15]-[17] and [21, 22] in the NLO approach to DIC process (1). This approach, which we will call "$1/\alpha_s$" approach, is motivated by large logarithms of Q^2 in the F_2^γ existing already in the PM. By expressing $\ln(Q^2/\Lambda_{QCD}^2)$ as $\sim 1/\alpha_s$ one treats the parton densities in the photon (and parton fragmentation into the photon) as proportional to α_{em}/α_s (see e.g. [3]-[5],[8, 9],[15]-[17] and [21, 22]). By applying this method to the DIC process, we see that the single resolved photon contribution to the cross section for the process $\gamma p \to \gamma X$ becomes of the same order as the Born term.The same is also observed for the double resolved photon contribution. Namely, we have for the Born, single and double resolved

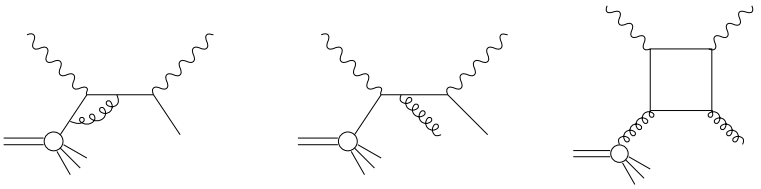

Figure 3. Examples of the virtual gluon (left) and real gluon (center) α_s corrections to the Born contribution. Also a box diagram is shown (right).

photon contributions:

$$1 \otimes [\alpha_{em}^2] \otimes 1 = \alpha_{em}^2, \quad \frac{\alpha_{em}}{\alpha_s} \otimes [\alpha_{em}\alpha_s] \otimes 1 = \alpha_{em}^2, \quad \frac{\alpha_{em}}{\alpha_s} \otimes [\alpha_s^2] \otimes \frac{\alpha_{em}}{\alpha_s} = \alpha_{em}^2.$$

In such counting, the same α_{em}^2 order contributions to the hadronic cross section are given by the direct Born process, single and double resolved photon processes although they correspond to quite different final states (observe a lack of the remnant of the photon in the direct process). Moreover, they constitute the lowest order (in the strong coupling constant) term in the perturbative expansion, actually the zeroth order, so the direct dependence of the cross section on the strong coupling constant is absent. Some of these terms correspond to hard processes involving gluons, still there are no terms proportional to α_s coupling!

In the "$1/\alpha_s$" approach the α_s correction to the Born cross section, the single and the double resolved photon contributions are included in the NLO calculation, since all of them give terms of the same order $\alpha_{em}^2\alpha_s$, see [15]-[17], [21, 22].

To summarize, the first approach starts with one basic, direct subprocess as in the PM (eq. 2), while the second approach considers three different types of subprocesses (as in the standard LL calculation). Obviously, some of the NNLO terms in the first method belong to the NLO terms in the second one.

In this paper we apply the first type of NLO approach to the DIC process, in particular we take into account the following subprocesses:
• the Born contribution (2) (fig. 1, left);
• the finite α_s corrections to the Born diagram (so-called K-term) from virtual gluon exchange, real gluon emission (fig. 3, left and center), and the process $\gamma g \to q\bar{q}\gamma$;
• two types of single resolved photon contributions, with resolved initial and final photons (fig. 2, left and center).

Besides the above full NLO set, we will include two terms of order $\alpha_{em}^2\alpha_s^2$ (formally from the NNLO set): the double resolved contributions (fig. 2, right) and the direct diagram (box) $\gamma g \to \gamma g$ [27] (fig. 3, right), since they were found to be large [3]-[8].

The cross section for the $\gamma p \to \gamma X$ scattering has the following form:

$$E_\gamma \frac{d^3\sigma^{\gamma p\to\gamma X}}{d^3p_\gamma} = \sum_b \int dx f_{b/p}(x,\bar{Q}^2)\frac{\alpha_s(\bar{Q}^2)}{2\pi^2\hat{s}}K_b +$$

$$+\sum_{abc}\int\frac{dz}{z^2}\int dx_\gamma\int dx f_{a/\gamma}(x_\gamma,\bar{Q}^2)f_{b/p}(x,\bar{Q}^2)\cdot D_{\gamma/c}(z,\bar{Q}^2)E_\gamma\frac{d^3\sigma^{ab\to cd}}{d^3p_\gamma}. \quad (4)$$

The first term is the K-term, and the second one stands for the sum over all other contributions including the Born term. The $f_{a/\gamma}$ ($f_{b/p}$) is a a (b)-parton distribution in the photon (proton) while the $D_{\gamma/c}$ is a c-parton fragmentation function. For the direct initial (final) photon, where $a=\gamma$ ($c=\gamma$), we take $f_{a/\gamma}=\delta(x_\gamma-1)$ ($D_{\gamma/c}=\delta(z-1)$) (the Born contribution is obtained for $a=\gamma$, $b=q$ and $c=\gamma$). The variables x_γ, x and z stand for the fraction of the initial photon, proton, and c-parton momenta taken by the a-parton, b-parton, and the final photon, respectively.

3. The isolation

In order to observe photons originating from a hard subprocess one should reduce backgrounds, mainly from π^0's and γ's radiated from final state hadrons. To achieve this, isolation cuts on the observed photon are introduced in experimental analyses. The isolation cuts are defined by demanding that the sum of transverse hadronic energy within a cone of radius R around the final photon, where the radius R is defined in the rapidity and azimuthal angle space, should be smaller than the final photon transverse energy multiplied by a small parameter ϵ: $\sum_{hadrons}E_{Th}<\epsilon E_{T\gamma}$. ‡

The simplest way to calculate the differential cross section for an isolated photon, $d\sigma_{isol}$, is to calculate the difference of a non-isolated differential cross section, $d\sigma_{non-isol}$, and a subtraction term, which corresponds to cuts opposite to the isolation cuts $d\sigma_{sub}$ [28]-[30], [15]: $d\sigma_{isol}=d\sigma_{non-isol}-d\sigma_{sub}$.

Note that in practice the isolation cuts are imposed only when calculating the K-term, and the contributions involving fragmentation function (resolved final photon). In calculating the subtraction term for the K-term we applied a small-δ approximation, see [29, 15] §. Presently we are working on calculations of the cross sections for the γ and γ+jet photoproduction using for a comparison the space slicing method [20], as in [17, 21, 22].

4. The results and comparison with data

We consider the production of photons with large transverse momentum, $p_T\gg\Lambda_{QCD}$, in the ep scattering, $ep\to e\gamma X$, at the HERA collider using the equivalent photon (Williams-Weizsäcker) approximation [33]:

$$d\sigma^{ep\to e\gamma X}=\int G_{\gamma/e}(y)d\sigma^{\gamma p\to\gamma X}dy, \quad (5)$$

‡ Some aspects of the QCD calculation of the isolated photon production are discussed in [31, 32].
§ This small-δ approximation seems to be an accurate analytic technique for including isolation effects in NLO calculations (also for $R=1$), see discussion in [17].

where y is (in the laboratory frame) a fraction of the initial electron energy taken by the photon [34]:

$$G_{\gamma/e}(y) = \frac{\alpha_{em}}{2\pi}\{\frac{1+(1-y)^2}{y}\ln[\frac{Q^2_{max}(1-y)}{m_e^2 y^2}] - \frac{2}{y}(1-y-\frac{m_e^2 y^2}{Q^2_{max}})\}, \quad (6)$$

with m_e being the electron mass. We assume Q^2_{max} equal to 1 GeV^2, as in the recent photoproduction measurements at the HERA collider. We neglect the large p_T photon emission from the electron [35].

The results for the non-isolated and isolated photon cross sections are obtained in NLO accuracy with additional NNLO terms, as discussed above. We take the HERA collider energies: E_e=27.5 GeV and E_p=820 GeV [12], and the p_T range of the final photon between 5 and 20 GeV (x_T from 0.03 to 0.13). The $\overline{\rm MS}$ scheme with a hard (renormalization, factorization) scale $\bar{Q}$=p_T (also $\bar{Q} = p_T/2$ and $2p_T$) has been applied. We assume the number of active (massless) flavors to be N_f=4 (and for comparison also N_f=3 and 5). The two-loop coupling constant α_s is used with Λ_{QCD}=0.365, 0.320 and 0.220 GeV for N_f=3, 4 and 5, respectively, as fitted by us to the experimental value of $\alpha_s(M_Z) = 0.1177$ [36].

We use the GRV parametrizations of the proton structure function (NLO and LO) [37], the photon structure function (NLO and LO) [38], and the fragmentation function (NLO) [39]. For comparison other parametrizations were also used: DO [4], ACFGP [8], CTEQ [40], MRST [41] and GS [42]. As reference we take the GRV NLO set of parton distributions [37]-[39], $N_f = 4$, $\Lambda_{QCD} = 320$ GeV and $\bar{Q} = p_T$.

4.1. Non-isolated versus isolated photon cross section

We have studied the p_T distribution for the produced final photon without any cut and found that it decreases by three orders of magnitude when p_T increases from 4 GeV to 20 GeV (not shown). Obviously the most important contribution is coming from the lowest p_T region, where the resolved photon processes dominate. The total NLO cross section integrated over p_T range from 5 to 10 GeV is equal to 226 pb, with individual contributions equal to: *Born* = 36.3%, *single resolved* = 35.1%, *double resolved* = 18.7%, *box* = 6.2%, *K-term*=3.9%, so the single resolved photon processes give a contribution comparable to the Born term. Also the double resolved photon processes are important. The direct box diagram ($\gamma g \to \gamma g$) gives 17% of the Born ($\gamma q \to \gamma q$) contribution. Such relatively large contribution is partially due to large gluonic content of the proton at small x_p.

The differential cross section for the final photon rapidity, $d\sigma/d\eta_\gamma$, for the non-isolated photon and for the photon isolated with various cones (various ϵ, R) was studied. The isolation cut suppresses the cross section significantly in the whole rapidity range (not shown). For ϵ=0.1 and $R = 1$ the suppression is 17-23% at rapidities $-1.5 < \eta_\gamma \leq 4$. ‖

‖ The positive rapidity points in the proton direction.

As expected, the cross section for fragmentation processes is strongly suppressed: after isolation it is lowered by a factor of 5. At the same time the QCD corrections to the Born diagram increase significantly, i.e. the contribution to the subtraction cross section, $d\sigma_{sub}$, due to these corrections is negative. The subtraction cross section, being a sum of negative QCD corrections and fragmentation contributions, is of course positive.

4.2. Other experimental cuts

In order to compare the results with data we fix R=1 and ϵ=0.1, which are the standard values used in both theoretical and experimental analyses, and consider other cuts imposed by the ZEUS group [12]. Two types of final state were measured in the ZEUS experiment: 1) an isolated photon with $-0.7 \leq \eta^{\gamma} \leq 0.9$ and $5 \leq p_T \leq 10$ GeV; 2) an isolated photon plus jet with the photon rapidity and transverse momentum as above, the jet rapidity in the range $-1.5 \leq \eta^{jet} \leq 1.8$, and the jet transverse momentum $p_T^{jet} \geq 5$ GeV. Here we compare our NLO predictions with the ZEUS data from the first type of measurements [12]. More results can be found in [19] and [20].

We have found (see [19]) that the cross section for a production of final γ is strongly reduced, by 30-85%, in the positive rapidity region due to the limited energy range, $0.2 \leq y \leq 0.9$ (see also [21, 22] for a similar conclusion). At negative rapidities the change due to the y-cut is weaker: 5-10% at $-1.2 < \eta_{\gamma} \leq -0.4$ and 10-30% at other negative rapidities. Note, however, that the Born term is reduced 3.5 times.

The role of various experimental cuts is illustrated in fig. 4, for the x_{γ} distribution. The small x_{γ} contributions are strongly, by two orders of magnitude, diminished by the photon rapidity cut. This shows that measurements at the central η^{γ} region ($-0.7 \leq \eta^{\gamma} \leq 0.9$) are not too sensitive to the small x_{γ} values in the photon and can not be used presently for constraining e.g. the gluon density in the photon.

4.3. The comparison with data

In fig. 5 (left) a comparison is made with ZEUS data for the p_T distribution for isolated γ for various N_f. Satisfactory agreement is obtained for $N_f = 4$ (and 5). Note the large difference between the results for N_f=4 and 3 due to the fourth power of electric charge. The rapidity distribution is shown in fig. 5(right), where a good description of the data is obtained for N_f=4 and 5 in the rapidity region $0.1 \leq \eta_{\gamma} \leq 0.9$. For $-0.7 \leq \eta_{\gamma} \leq 0.1$ our predictions lie mostly below the experimental points. This disagreement between predicted and measured cross sections is observed also for other theoretical calculations (LG,FGH) and for Monte Carlo simulations [12]. In fig. 5(right) we present separately an effect due to the box subprocess (for $N_f = 4$). It is clear that the box term enhances considerably the cross section in the measured rapidity region (by $\sim 10\%$). The double resolved photon contribution is also sizeable, although roughly two times smaller than the box one. Both these α_s^2 contributions improve description of the data.

The predictions obtained using three different NLO parton densities in the photon (ACFGP [8], GRV [38] and GS [42]) are presented for $N_f = 4$ in fig. 6 for $\bar{Q} = p_T$

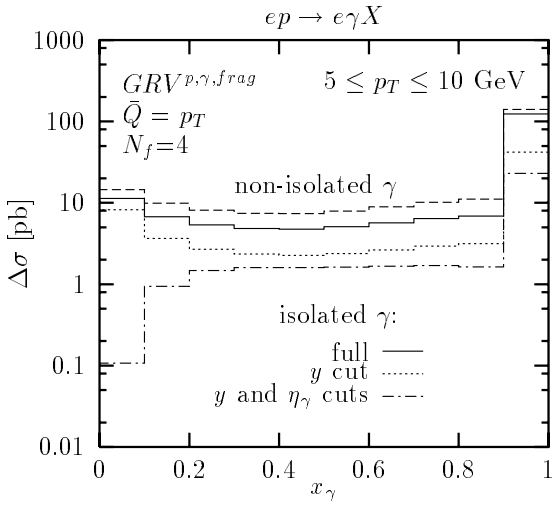

Figure 4. The cross section in x_γ bins the length 0.1. The results for non-isolated γ are shown (dashed line). The solid line represents results for isolated γ with $\epsilon = 0.1$ and $R = 1$. Results with additional cuts in the isolated γ cross section are shown with: dotted line ($0.2 \le y \le 0.9$) and dot-dashed line ($0.2 \le y \le 0.9$, $-0.7 \le \eta_\gamma \le 0.9$).

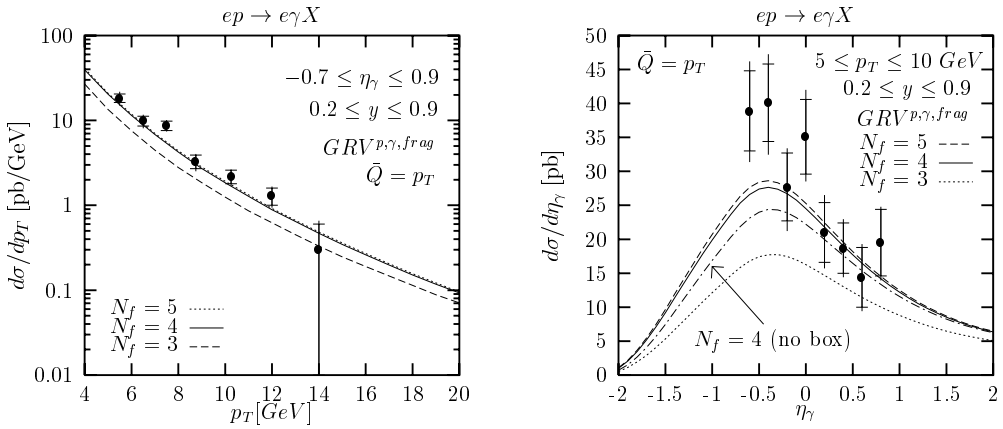

Figure 5. The results for isolated γ for: $N_f = 3$ (dashed lines), 4 (solid lines) and 5 (dotted lines), compared to the ZEUS data [12]. The $d\sigma/dp_T$ as a function of the photon transverse momentum (left) and $d\sigma/d\eta_\gamma$ as a function of the photon rapidity η_γ (right); the result without the box contribution is also shown for $N_f = 4$ (dot-dashed).

(left) and for $\bar{Q} = 2p_T$ (right) together with the ZEUS data [12]. The results based on ACFGP and GRV parametrizations differ by less than 4% at rapidities $\eta_\gamma < 1$ (at higher η_γ the difference is bigger), and both give good description of the data in the rapidity range $0.1 \le \eta_\gamma \le 0.9$ (for $\bar{Q} = p_T$ and $\bar{Q} = 2p_T$). For $-0.7 \le \eta_\gamma \le 0.1$ none of the predictions is in agreement with the measured cross section. For $\bar{Q}$=p_T (fig. 6 left) the GS distribution leads to results considerably below the ones obtained using ACFGP and GRV densities, especially in the rapidity region from roughly -1 to 1. This is due to a different treatment of the charm quark in the photon, namely in the GS approach the charm quark is absent for $\bar{Q}^2$ below 50 GeV^2 - contrary to GRV and ACFGP parametrizations where the charm threshold occurs at lower $\bar{Q}^2$. All the

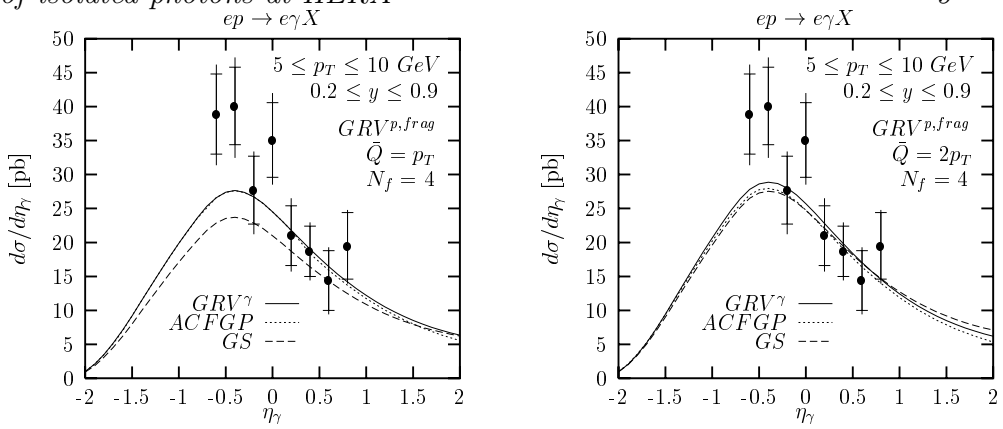

Figure 6. The $d\sigma/d\eta_\gamma$ for isolated γ compared to the ZEUS data [12]. Three different NLO parton distributions for γ: ACFGP [8] (dotted line), GRV [38] (solid line) and GS [42] (dashed line). $\bar{Q} = p_T$ (left) and $\bar{Q} = 2p_T$ (right).

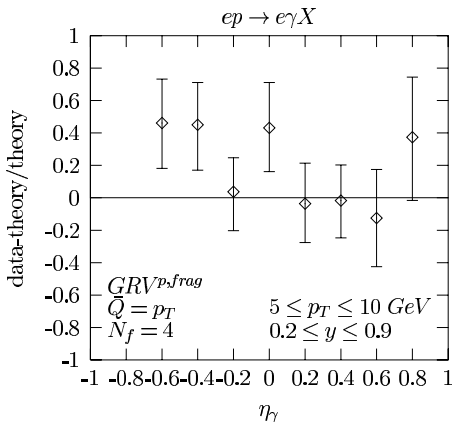

Figure 7. (Data-theory)/theory for GRV parton parametrizations for the initial and final photons and the proton with ZEUS data from [12].

considered parton distributions give similar descriptions of the data when the scale is changed to $\bar{Q} = 2p_T$, since then $\bar{Q}^2$ is always above 50 GeV^2. The (data-theory)/theory for the same cross section for the reference set (GRV) of parton parametrizations is presented in fig. 7. In fig. 8 our predictions are compared to the ZEUS data divided into three ranges of y. Clearly the discrepancy discussed above between the data and the predictions for $\eta^\gamma < 0.1$ is coming mainly from the low y region, $0.2 < y < 0.32$. In the high y region, $0.5 < y < 0.9$, a good agreement is obtained for the whole measured rapidity region. This is not the case for LG and FGH results which are in disagreement even for large y (mainly for rapidities above 0.1, see below).

We have also studied the dependence of our results on the choice of the parton distributions in the proton and parton fragmentation into the photon (not shown), and a small sensitivity was found. Only at minimal ($\eta_\gamma < -1$) and maximal ($4 < \eta_\gamma$) rapidity values this difference is larger, being at a level of $3.5 - 8\%$.

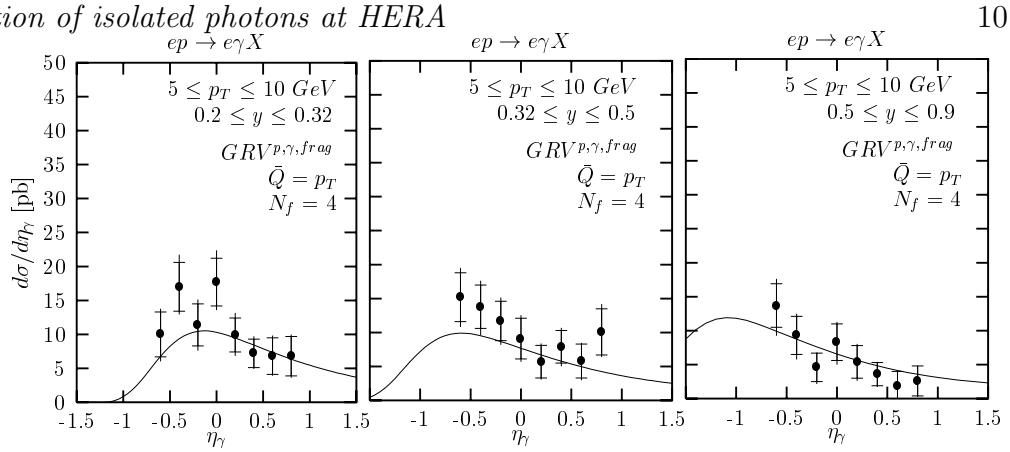

Figure 8. The results for three ranges of y: $0.2 < y < 0.32$, $0.32 < y < 0.5$ and $0.5 < y < 0.9$, compared to the ZEUS data [12].

5. The theoretical uncertainties and comparison with other NLO analyses

In order to estimate the contribution due to missing higher order terms, we have studied the influence of the choice of the $\bar{Q}$ scale for the η_γ distribution. Some of the results can be found in fig. 6 for the GRV and ACFGP parton parametrizations. Around the maximum of the cross section at rapidities $-1 \le \eta_\gamma \le 0$ changing $\bar{Q}$ scale from $p_T/2$ to $2p_T$ leads to differences 4-6%. This small sensitivity of the results to the change of the scale is important since it indicates that the contribution from neglected NNLO and higher order terms is not significant. Note that individual contributions are strongly dependent on the choice of $\bar{Q}$, e.g. results for the single resolved processes vary by ±10-20% at rapidities $\eta_\gamma \le 1$. Results are much more stable only when the sum of resolved processes and QCD corrections is considered. These results lead to the expectation that our prediction should not differ too much from results based on larger set of diagrams.

As we discussed in Sec. 2, our NLO calculation of the DIC process differs from the "$1/\alpha_s$"-type NLO analysis presented in ref. [15]-[17] and [21, 22] by a set of diagrams included in the calculation. We do not take into account α_s corrections to the single and double resolved processes, which are beyond the NLO accuracy in our approach. On the other hand, we include the box diagram neglected in [15]-[17], which however is taken into account in the FGH analysis [21, 22]. (The double resolved subprocesses are included in all mentioned analyses.)

We compare now our results and the results of the LG calculation [17] (using N_f=4 and $\bar{Q} = p_T$) for the isolated final photon (R=1, ϵ=0.1) in the kinematical range as in the ZEUS analysis [12] (i.e. for $-0.7 \le \eta^\gamma \le 0.9$ and $0.2 \le y \le 0.9$), see fig. 9(left). In fig. 9(right) a comparison is made for the FGH results [21] and the same data. The LG predictions (and FGH results) for $d\sigma/dp_T$ (with GRV parton parametrization) are about 20% higher than ours in the presented range of transverse momentum, $4 \le p_T \le 20$ GeV. For $d\sigma/d\eta^\gamma$ cross section (with $5 \le p_T \le 10$ GeV) the biggest differences between our and LG predictions are at large y range, as can be seen in fig. 10 (left). For a y range limited to low values only, $0.2 < y < 0.32$, the LG cross section is higher than

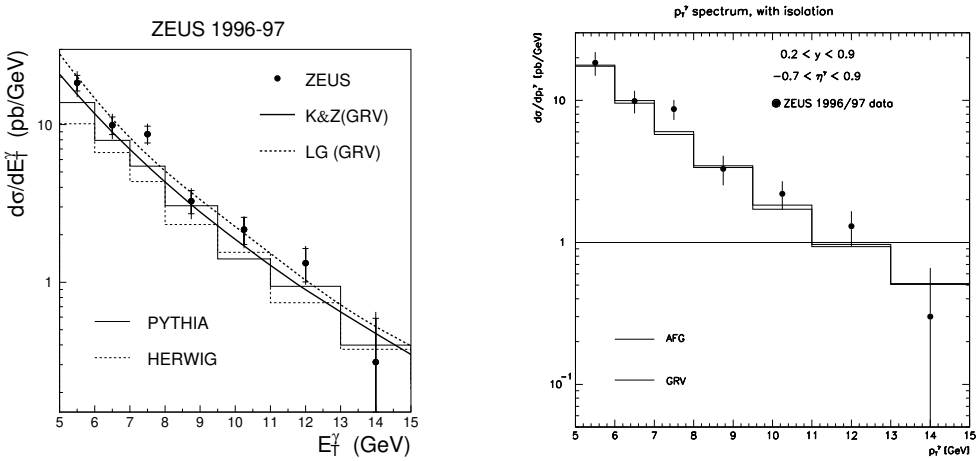

Figure 9. The comparison of the data for the p_T distribution (from [12]) with PYTHIA and HERWIG Monte Carlo predictions and with our results and LG ones based on GRV parametrizations (left). The same data in comparison with the FGH results (left, from [21]).

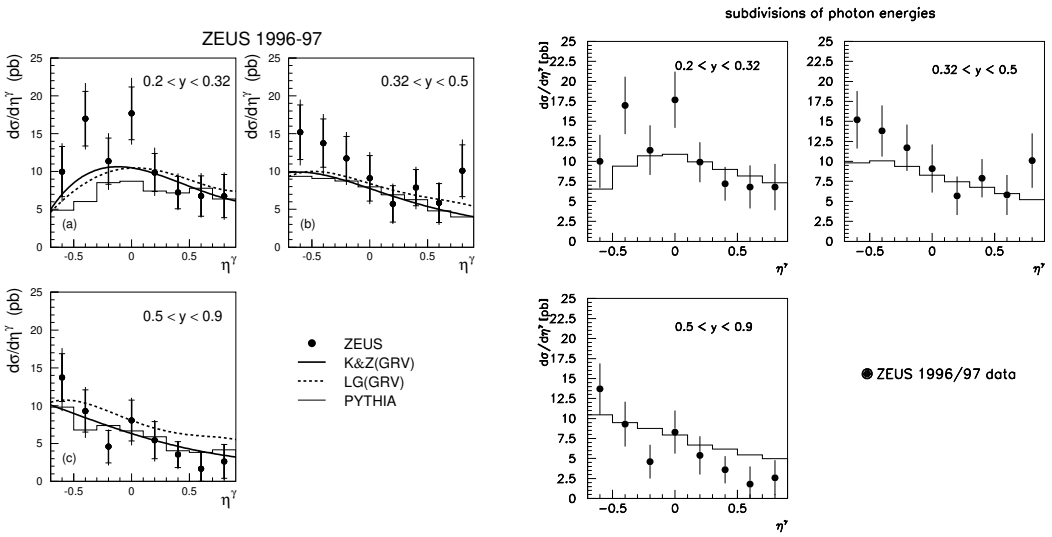

Figure 10. The comparison with data for the rapidity distribution of the final photon for three ranges of y (as in fig.7) of PYTHIA prediction, our results and LG results (for GRV), (left, (from [12])) and similar comparison between data and FGH results, from [21] (right).

ours by up to 20% at positive η_γ, while at negative η_γ it is lower by up to 10%. For large y values, $0.5 < y < 0.9$, where our predictions agree with the data, the LG results are higher than ours by up to 80% (at $\eta_\gamma = 0.9$). Not only the LG predictions are too high as compared to the data in the forward direction, a similar effect especially for large y is seen in fig. 10(right), where the FGH results are compared with data. Our predictions as we discussed above are close to the data for η_γ above 0.1, see figs. 7, 8 and 10(left).

6. Summary

Results of the NLO calculation, with additional NNLO contributions from double resolved photon processes and box diagram, for the isolated γ production in the DIC process at HERA are presented ¶. The role of the kinematical cuts used in the ZEUS measurement [12] are studied in detail.

The results obtained using GRV parametrizations agree with the data in shape and normalization for the p_T distribution. For the η^γ distribution a good description of the data is obtained for $\eta^\gamma > 0.1$, while for $\eta^\gamma < 0.1$ the data usually lie above the predictions. This discrepancy arises mainly from the low y region, $0.2 \leq y \leq 0.32$. The beyond NLO terms, especially a box contribution, improve the description of the data.

We have studied the theoretical uncertainty of the results due to the choice of the renormalization/factorization scale: $\bar{Q} = p_T/2, p_T, 2p_T$. At high rapidities $\eta_\gamma > 3$, where the cross section is small, this uncertainty is 10-30%. In a wide range of rapidities, $-2 \leq \eta_\gamma \leq 2$, the dependence on the $\bar{Q}$ scale is small, below 6%. Since we include some NNLO diagrams in our NLO calculation, this stability of the predictions versus the change of the scale is especially important. The weak dependence on the $\bar{Q}$ scale and differences between LL and NLO predictions not being large (below 20%) allow to conclude that theoretical uncertainties of our NLO calculations for production of an isolated photon in the DIC process at HERA are relatively small.

We compared our results with the "$1/\alpha_s$" NLO calculations by LG and FGH which are based on a different set of subprocesses. The cross section $d\sigma/dp_T$ obtained by LG is about 20% higher than ours (for GRV photonic parton distributions), the FGH prediction is closer to ours than the LG one, it lies between KZ and LG curves. For the cross section $d\sigma/d\eta_\gamma$ the difference between our results and LG/FGH ones is up to 35% at $\eta_\gamma = 0.9$. The highest differences are present for high y values only, $0.5 < y < 0.9$, where on the other hand our predictions are in agreement with the data. At low y range, $0.2 < y < 0.32$, differences between our calculation and calculations done by LG and FGH are smaller and none of them describe the data well for rapidities below 0.1.

7. Acknowledgments

I would like to thank Andrzej Zembrzuski for his help in preparing this talk and valuable discussions. The discussion with Jiri Chyla, Andreas Vogt, Bernd Kniehl, Michel Fontannaz and Werner Vogelsang is acknowledged. I would like to thank the organizers for this stimulating workshop.
Supported in part by Polish State Committee for Scientific Research, grants number 2P03B05119 (2000-2001), and by European Commission 50th framework contract HPRN-CT-2000-00149.

¶ Our fortran code is available upon request from azem@fuw.edu.pl.

References

[1] J. D. Bjorken and E. A. Paschos, Phys. Rev. **185** (1969) 1975
[2] T. Tu, C. Wu, Nucl. Phys. B **156** (1979) 493
[3] M. Fontannaz and D. Schiff, Z. Phys. C **14** (1982) 151
[4] D. W. Duke and J. F. Owens, Phys. Rev. D **26** (1982) 1600; Err: Phys. Rev. D **28** (1983) 1227
[5] P. Aurenche, A. Douiri, R. Baier, M. Fontannaz and D. Schiff, Z. Phys. C **24** (1984) 309
[6] M. Krawczyk, Acta Physica Polonica B **21** (1990) 999
[7] A. C. Bawa, M. Krawczyk and W. J. Stirling, Z. Phys. C **50** (1991) 293 A. C. Bawa and M. Krawczyk, Phys. Lett. B **262** (1991) 492; Proc. "Physics at HERA", Hamburg 1991, p. 579; M. Krawczyk, *proc. 27th Rencontres de Moriond: QCD and High Energy Hadronic Inter., Les Arcs, France, 1992, p. 69*;
[8] P. Aurenche, P. Chiappetta, M. Fontannaz, J. P. Guillet and E. Pilon, Z. Phys. C **56** (1992) 589
[9] L. E. Gordon and J. K. Storrow, Z. Phys. C **63** (1994) 581
[10] ZEUS Coll., J. Breitweg et al., Phys. Lett. B **413** (1997) 201
[11] ZEUS Coll., *Subm. to the XXIXth Inter. Conf. on High-Energy Physics (ICHEP 98), Vancouver, Canada, 1998, abstract 815*
[12] ZEUS Coll., J. Breitweg et al., Phys. Lett. B **472** (2000) 175
[13] S. Chekanov *et al.* [ZEUS Collaboration], Phys. Lett. B **511** (2001) 19 [arXiv:hep-ex/0104001].
[14] H1 Coll., *Subm. to the Inter. Europhysics Conf. on High Energy Physics, HEP97, Jerusalem, Israel, 1997, abstract 265*
[15] L. E. Gordon and W. Vogelsang, Phys. Rev. D **52** (1995) 58
[16] L. E. Gordon and W. Vogelsang, hep-ph/9606457,
[17] L. E. Gordon, Phys. Rev. D **57** (1998) 235
[18] M. Krawczyk and A. Zembrzuski, hep-ph/9810253, IFT 98/12, in proc. *the XXIXth Inter. Conf. on High Energy Physics, ICHEP'98, Vancouver, Canada, p. 897*
[19] M. Krawczyk and A. Zembrzuski, arXiv:hep-ph/0105166, to appear in Phys. Rev. D **64** (2001)
[20] A. Zembrzuski, in preparation
[21] M. Fontannaz, J. P. Guillet and G. Heinrich, Eur. Phys. J. C **21** (2001)303 [arXiv:hep-ph/0105121].
[22] M. Fontannaz, J. P. Guillet and G. Heinrich, arXiv:hep-ph/0107262.
[23] G. Kramer, D. Michelsen and H. Spiesberger, Eur. Phys. J. C **5** (1998) 293; A. Gehrmann-De Ridder, G. Kramer and H. Spiesberger, Phys. Lett. B **459** (1999) 271; Eur. Phys. J. C **11** (1999) 137; Nucl. Phys. B **578** (2000) 326
[24] J. Chýla, JHEP 0004 (2000) 007; hep-ph/9811455; hep-ph/0010140; hep-ph/0010309
[25] M. Krawczyk, unpublished
[26] J. Żochowski, *"The α_S corrections in Deep Inelastic Compton Scattering", MS Thesis, 1992*
[27] B. L. Combridge, Nucl. Phys. B **174** (1980) 243
[28] E. L. Berger and J. Qiu, Phys. Lett. B **248** (1990) 371; Phys. Rev. D **44** (1991)2002
[29] L. E. Gordon and W. Vogelsang, Phys. Rev. D **50** (1994) 1901
[30] M. Glück, L. E. Gordon, E. Reya and W. Vogelsang, Phys. Rev. Lett. **73** (1994) 388
[31] E. L. Berger,X. Guo and J. Qiu, Phys. Rev. Lett. **76** (1996) 2234; Phys. Rev. D **54** (1996)5470;
[32] P. Aurenche et al. Phys. Rev. D **55** (1997) R1124; S. Catani, M. Fontannaz and E. Pilon, Phys. Rev. D **58** (1998) 094025
[33] C. F. von Weizsäcker, Z. Phys. **88** (1934) 612; E. J. Williams, Phys. Rev. **45** (1934) 729; E.J. Williams, Kgl. Danske Vidensk. Selskab. Mat.-Fiz. Medd. 13 (1935) N4
[34] V. M. Budnev, I. F. Ginzburg, G. V. Meledin and V. G. Serbo, Phys. Rep. **15** (1975) 181; R. Nisius, Phys. Rep. **332** (2000) 165
[35] U. A. Jezuita-Dąbrowska, *"The polarization states of the virtual photon in $ep \to e\gamma X$ at HERA", MS Thesis, 1999*
[36] O. Biebel, P. A. Movilla Fernandez, S. Bethke and the JADE Coll., Phys. Lett. B **459** (1999) 326
[37] M. Glück, E. Reya and A. Vogt, Z. Phys. C **67** (1995) 433

[38] M. Glück, E. Reya and A. Vogt, Phys. Rev. D **45** (1992) 3986; Phys. Rev. D **46** (1992) 1973
[39] M. Glück, E. Reya and A. Vogt, Phys. Rev. D **48** (1993) 116
[40] H.L. Lai et al., Phys. Rev. D **55** (1997) 1280
[41] A. D. Martin, R. G. Roberts, W. J. Stirling and R. S. Thorne, Eur. Phys. J. C **4** (1998) 463
[42] L. E. Gordon and J. K. Storrow, Nucl. Phys. B **489** (1997) 405